Hydrological impacts of climate change on small ungauged catchments-results from a GCM-RCM-hydrologic model chain

Aynalem T. Tsegaw[1], Marie Pontoppidan[2], Erle Kristvik[1], Knut Alfredsen[1] , Tone M. Muthanna[1]

[1] Department of Civil and Environmental Engineering, Norwegian University of Science and Technology (NTNU), S.P. Andersensvei 5, N-7491, Trondheim, Norway.

[2] NORCE Norwegian Research Centre, Bjerknes Centre for Climate Research, Bergen, Norway.

Correspondence to: Aynalem T. Tsegaw (aynalemtassachew1982@gmail.com)

Abstract. Climate change is one of the greatest threats to the World's environment. In Norway, a change in climate will strongly affect the pattern, frequency and magnitudes of stream flows. However, it is highly challenging to quantify to what extent the change in climate will affect flow patterns and floods from small rural catchments due to unavailability or inadequacy of hydro-meteorological data for the calibration of hydrological models and tailoring methods to a small-scale level. To provide meaningful climate impact studies at small catchments, it is therefore beneficial to use high spatial and temporal resolution climate projections as input to a high-resolution hydrological model. Here, we use such a model chain to assess the impacts of climate change on flow patterns and frequency of floods in small ungauged rural catchments in western Norway. We use a new high-resolution regional climate projection, with improved performance regarding to the precipitation distribution, and a regionalized hydrological model (Distance Distribution Dynamics) between the reference (1981-2011) and future (2070-2100) periods. The flow-duration curves of all study catchments show more wet periods in the future than during the reference period. The results also show that in the future period, the mean annual flow increases by 16% to 33%. The mean annual maximum floods increase by 29% to 38%, and floods of 2 to

200 years return periods increase by 16% to 43%. The results are based on the RCP8.5 emission scenario from a single climate model simulation tailored to western Norway and the Bergen region and the results should be interpreted in this context. The results should therefore be seen in consideration of other scenarios for the region to address the uncertainty. Nevertheless, the study increases our knowledge and understanding on the hydrological impacts of climate change on small catchments at the Bergen area in the western part of Norway.

1 Introduction

Climate change is one of the greatest threats to human existence, economic activity, ecosystems and civil infrastructures (Kim and Choi, 2012). The climate change risks depend on: the magnitude of warming, rate of warming, geographic location, levels of development, vulnerability, and on the choices and implementation of adaptation and mitigation options (IPCC, 2018). The trends of changes in different parts of Europe vary considerably because of changes in large-scale atmospheric circulation or local orographic circulation (Eisenreich et al., 2005, Hattermann et al., 2007).

Changes in temperature and precipitation and the shift in winter precipitation from snow to rain will be crucial in studying impacts of climate change on hydrology of a catchment. These changes influence the hydrological regime of a stream, and the most serious and widespread potential impact of the changes is flooding (Baltas, 2007, Richardson, 2002, Thornes, 2001). The Blöschl et al. (2019) study shows that increasing autumn and winter rainfall resulted in increasing floods in Northern Europe. In Norway, the average annual temperature and precipitation are expected to

increase by 3.8 °C to 6.2 °C and 7% to 27% respectively by the end of the century using RCP8.5 emission scenario (Hanssen-Bauer et al., 2015). The largest increases in precipitation are mostly expected during the autumn and winter months and will in turn impact the magnitude and in some cases the seasonality of peak runoff and floods. A climate impact study at Sogn and Fjordane county of Norway shows that flood peaks shift from summer to autumn for the future scenario (Chernet et al., 2014), and Donnelly et al. (2017) studied climate change impacts on European hydrology and found that in the Norwegian region, climate change will strongly affect the hydrological cycle in the future period. Outside Norway, authors have reported that the frequency and magnitude of flows are being affected by the changes in climatic conditions (Alfieri et al., 2015; Madsen et al., 2014; Mallakpour & Villarini, 2015; Rojas et al., 2013). Climate change adverse results upon streamflow regimes worldwide (Pumo et al., 2016), calls for attention of the impact study on a local scale.

Projected increase in the frequency and intensity of heavy localized precipitation events, based on climate models, contributes to increasing in precipitation-generated local flooding, and an increase in local sudden flooding is causing significant danger and loss of life and property (Borga et al., 2011, Kundzewicz et al., 2014). Local sudden floods (flash floods) usually occur in small catchments (e.g., catchments less than 100 – 1000 km^2). This type of flood event is usually short in duration, but it is usually connected with severe damage (Menzel et al., 2006). Studies show that the probability and magnitude of hazardous heavy precipitation events have been increasing in several European regions e.g., (Golz et al., 2016). Heavy localized precipitation could be caused by low pressure systems (e.g., western Norway (Azad and Sorteberg, 2017)) or because of prevailing convective precipitation at hilly or mountainous areas.

A quantitative analysis of the impacts of climate change on flooding conditions requires simulations in a climatological-hydrological system. The models on which the simulations are based should give an adequate representation of the system dynamics relevant for different types of flow (e.g. floods) generation (Menzel et al., 2006). Hydrological models provide the means to conceptualize and investigate the relationship between climate (e.g. precipitation and temperature) and water resources (e.g. low flows and floods) of a region to assess the likely effects of climate change and propose appropriate adaptation strategies (Baltas, 2007). The results of regional climate impact studies help in proposing adaptation measures to local climatic, geographic, economic and social conditions (Hattermann, 2009, Krysanova et al., 2008). Hydrological impact of climate change is generally performed by following a sequence of steps from global and regional climate modelling, through data tailoring (downscaling and bias-adjustment) and hydrological modelling (Olsson et al., 2016).

Climate impact assessment on hydrology of small ungauged catchments using continuous hydrological modelling is challenging because of unavailability or inadequacy of hydro-meteorological data for calibration of hydrological models, short response time of the catchments, difficulty in describing local hydrological processes and coarse resolution of climate models. The challenge in coarse spatial resolution of climate models is due to poor representation of precipitation which is inadequate for assessment of impacts on smaller catchments (Quintero et al., 2018). For example, Pontoppidan et al. (2017) showed that during a flooding event in western Norway, the regional model simulated observed rainfall considerably better with a grid spacing of 3 km compared to a grid spacing of 9 km due to the complex terrain in the area. Therefore, to provide a meaningful climate impact result at small catchments, it is necessary to use high spatial

and temporal resolutions of projected climate data as forcing in high resolution hydrological models (Lespinas et al., 2014; López-Moreno et al., 2013; Reynolds et al., 2015; Tofiq & Guven, 2014). Current efforts of coordinated regional downscaling in Europe (EURO-CORDEX e.g. (Jacob et al., 2014; Kotlarski et al., 2014)) are performed on a 0.11° grid, however a new high-resolution regional downscaling with improved representation of local precipitation distribution for southern Norway is available (Pontoppidan et al., 2018), but has yet to be included in a full hydrological model chain.

To solve the challenge related to lack of availability of a properly calibrated high-resolution hydrological model at ungauged small rural catchments in Norway, a predictive tool has been developed and tested. Tsegaw et al. (2019a) calibrated and validated Distance Distribution Dynamics (DDD) hydrological model at forty-one gauged small rural catchments in Norway with hourly temporal resolution. For predicting flow at ungauged catchments, the DDD model parameters have been regionalized using three methods of regionalization (multiple regression, physical similarity and combined method) and the methods have been tested on seven independent catchments. The finding shows that the combined method performs the best of all the methods in predicating flow. Even if the DDD model predicts flow at ungauged catchments satisfactory ($0.5 \leq$ Kling-Gupta Efficiency < 0.75), the model underestimates most of the observed flood peaks. To improve the prediction of observed floods, a dynamic river network method has been introduced and implemented in DDD (Tsegaw et al., 2019b). This improved setup has been used in this study where the general objective is to assess the hydrological impacts of climate change on small ungauged catchments using a novel model chain consisting of a high resolution, bias corrected dynamical downscaled climate scenario and the improved DDD model. We specifically focus on:

i. Assessing the impacts of climate change on the changes of flow patterns at ungauged small rural catchments around Bergen, Norway.

ii. Assessing impacts of climate change on the pattern and frequency of floods in ungauged small rural catchments around Bergen, Norway.

2 Data and methods

2.1 Study area

The Bergen area is known for its wet climate. The location is in the south western Norway (60N,5E) and coastal climate and pronounced topography. For the normal period of 1961-1990, statistical reports show an annual precipitation of 2250 mm (Florida weather station) and typically precipitation occurs 243 days every year (i.e. days with 0.1 mm or more precipitation) (Kristvik and Riisnes, 2015). The region is mostly affected by orographic precipitation, which is produced when humid air from the Northern Sea is lifted as it moves over the mountain range. The air rises and cools, forming clouds that typically precipitates upwind of the mountain ridge. Particularly, prominent mountains oriented across the wind gradient receive the heaviest precipitation. This causes major variations in precipitation loads, even within small distances (Kristvik and Riisnes, 2015).

Floods in south western part of Norway (where Bergen is located) are mainly caused by heavy rainfall during the autumn season (Roald, 2008). The Norwegian Center for Climate Services report (Climate in Norway 2100) pointed out that in river systems, dominated by rain floods, the magnitude of floods is projected to increase by almost 60% (RCP8.5) towards the end of the century, and more frequent and stronger intense rainfall events may in the future give special challenges in small, steep rivers which receive their flows from small catchments (Hanssen-Bauer et al., 2015). Vormoor et al (2015) found that autumn/winter events become more frequent by

2099, which leads to an intensification of the current autumn/winter flood regime for the coastal catchments in Norway. Blöschl et al. (2017) studied the impacts of climate change on shifting the timing of European floods using observed floods and found that in the south western part of Norway, 50% of the stations show a shift towards later floods (at the end of a year) by more than +8 days per 50 years.

Six ungauged small rural catchments, located in western Norway around Bergen city, are used in this study. The catchments characteristics data are taken from http://nevina.nve.no/ and http://www.statenskartverk.no/. The definition of small rural catchments is based on the report of Fleig and Wilson (2013) with an upper area limit of 50km^2. The catchments are selected for the impact study because there are critical infrastructures (e.g. culverts, bridges and buildings) at the outlet of the catchments which could be damaged by floods in the future period. We selected three catchments with bare mountain dominated (>50%) and three catchments with forest dominated (>50%) land uses to include diverse land uses in the study. The locations and observed river networks of the selected catchments are depicted in Fig. 1. The catchment descriptors (CDs) and outlet coordinates of each study catchment are presented in Table 1.

2.2 Climate, topography and land use data

2.2.1 Climate data and bias correction

The precipitation and temperature data used to drive the hydrological model are obtained from a simulation performed by the Weather Research and Forecasting model (WRF) version 3.8.1 (Skamarock et al., 2008). The model is non-hydrostatic and widely used for weather forecasting and research purposes. This RCP 8.5 scenario climate projection is unique because of its high

spatial grid resolution of 4 km x 4 km. To our knowledge, no other convective permitting, century-long, dynamically downscaled climate projection is available for Norway. Precipitation and temperature variables are available every 3 hours. However, regional models, as WRF, inherit biases from the boundary conditions used to drive the model. These biases may lead to misrepresentation of important features in the models, e.g. the known bias of the North Atlantic storm track (Zappa et al., 2013) leads individual storms into central Europe instead of a more northern path along the Norwegian coast as observations suggest. Therefore, the global climate model NorESM1-M (r1i1p1) used as forcing data at the boundaries in WRF was bias corrected before the regional downscaling. We followed the approach of Bruyère et al. (2015) and corrected the monthly mean values towards the monthly mean of the reanalysis ERA-Interim (Dee et al., 2011). The correction was performed for the skin temperature and the three-dimensional pressure, humidity, temperature and the wind components. The correction of the driving fields led to a more realistic representation of the North Atlantic storm track and the precipitation distribution in the regional model simulation (Pontoppidan et al., 2018).

Bias correction is an often-used method to address systematic model errors. Many studies apply a correction towards observation on variables as temperature and precipitation via a choice of distribution mapping towards observations. Normally this is performed on the regional climate model output (e.g. Muerth et al., 2013; Tramblay et al., 2013). Such posterior bias correction highly constrain the model output and the use of such have been questioned (Maraun, 2016; Maraun et al., 2017). Correcting variables individually may violate physical consistency because it tampers with known physical dependencies. Alternatively, bias correction can be applied upstream, i.e. on the global climate model before it is used as driving data for a regional model. In principle, this

will allow the interior of the regional model to adjust to any physical inconsistencies applied at the boundaries and develop a physical consistent climate within the model domain. Such an approach is widely used in a "storyline" approach where one add a climate change signal to reanalysis data before the downscaling (e.g. Rasmussen et al., 2011; Schär et al., 1996). However this pseudo global warming method also have caveats; it assumes that the climate variability is stationary in time, an assumption which have been widely questioned (Christensen et al., 2008; Maraun, 2012; Vannitsem, 2011). Instead we use a method that corrects the global climate model's monthly mean towards the reanalysis monthly mean. By doing so we overcome the stationary assumption because we retain the variability from the global model instead of limiting the variability to the reanalysis.

We bias corrected the global climate model driving data prior to the dynamical downscaling, leading to physical consistency in the interior domain, and a potential gain from the increased horizontal resolution. The approach showed improved precipitation representation in Australia (Rocheta et al., 2017), in North American climate (Wang & Kotamarthi, 2015; Xu & Yang, 2012, 2015) and in hurricane representation along the US east coast (Bruyère et al., 2014). In Norway the upstream bias correction led to a better represented North Atlantic storm track and an improved spatial precipitation distribution (Pontoppidan et al., 2018).

Mathematically the bias correction was performed following the anomaly approach (Bruyere et al., 2015). The reference period was selected to be a 30-year period from 1981 to 2010 and we adjusted the monthly NorESM1-M mean towards the monthly ERA-Interim (Dee et al., 2011) mean. For the reference period the 6-hourly NorESM1-M input data were split into a monthly

mean term and the deviation from this. For the future period the 6-hourly NorESM1-M input data were split into the monthly mean from the reference period and the deviation from this, leaving the climate change signal and the non-stationary variability in the deviation term. The new bias-corrected NorESM1-M data were then calculated by adding the monthly mean from the reanalysis product and the GCM deviation term. As opposed to the pseudo global warming method this approach ensured that the experiment retained the variability of the driving climate model. The bias correction equations are as follows:

$$ERAI_{ref} = ERAI_{ref} + ERAI' \quad (1)$$

$$GCM = GCM_{ref} + GCM' \quad (2)$$

$$GCM_{BC} = ERAI_{ref} + GCM' \quad (3)$$

where the mean terms are from the 30-year reference period and the deviation is the deviation from the refence period mean.

Bruyere et al. (2014) investigated the effect of bias correcting single and multiple variables. The conclusion was that the best results were obtained when a multivariate bias correction was performed. Therefore, we bias corrected the three-dimensional wind components, the temperature, the relative humidity, and the pressure fields in addition to the two-dimensional sea surface temperature fields in our driving data.

2.2.2 Topographical and land use data

The DDD model parameters, which do not need regionalization, are derived from an analysis of topographical and land use data of a catchment using GIS. The source of the topography and land use data is the Norwegian Mapping Authority (http://www.statenskartverk.no/).The 10m x 10 m DEM, the river network and the 1: 50 000 scale land use data have been retrieved and used in the study. The DEM has been re-conditioned to the naturally occurring river network using the Arc-hydro tool to create a hydrologically correct terrain model that can improve the accuracy of watershed modeling (Li, 2014). The re-conditioned DEM is further used to determine the distance distributions of hill slopes and river networks as needed by DDD.

2.3 DDD hydrological model

2.3.1 General description of the model

The Distance Distribution Dynamics (DDD) hydrological model is developed by Skaugen and Onof (2014) and currently runs operationally with daily and 3-hourly time steps at the Norwegian flood forecasting service. The model is semi-distributed conceptual and applicable for catchments ranging from small to large and temporal resolutions ranging from low to high. It has two main modules: the subsurface and the dynamics of runoff. The volume capacity of the subsurface water reservoir is shared between a saturated zone and an unsaturated zone. The volume of the saturated zone and the unsaturated zone are inversely related i.e. the higher the unsaturated zone volume, the lower the saturated zone (Skaugen and Mengistu, 2016, Skaugen and Onof, 2014). The dynamics of runoff in DDD has been derived from the catchment topography using a GIS combined with runoff recession analysis. In DDD, the distribution of distances between points in the catchment and their nearest river reach (distance distributions of a hillslope) is the basis for

describing the flow dynamics of the hillslope. The distribution of distances between points in the river network and the outlet forms the basis for describing the flow dynamics of the river network. The hillslope and river flow dynamics of DDD are described by unit hydrographs (UHs) which are derived from distance distributions and celerity using a GIS and recession analysis respectively (Skaugen and Mengistu, 2016, Skaugen and Onof, 2014). Figure 2 shows the structure of the DDD model.

2.3.2 Dynamic river network method in DDD

Dynamic river networks and hence dynamic overland unit hydrographs are introduced and implemented in the DDD model to improve the simulation of floods (Tsegaw et al., 2019b). The mean of the distribution of distances from a point in the catchment to the nearest river reach (D_m) becomes dynamic in the dynamic river network method. Therefore, we need to estimate the dynamic D_m from the relation between upstream critical supporting area (A_c) i.e. the area needed to initiate and maintain streams and D_m using GIS and python script as shown in Eq.(4). The coefficients (a and b) are estimated for each study catchments and presented in Table 2. The calibration parameter of the dynamic river network routine in DDD is critical flux (F_c) and is estimated by regional regression in this study.

$$D_m = aA_c^{\boldsymbol{b}} \qquad (\mathbf{4})$$

2.3.3 Model parameters and regionalization

The DDD model parameters are divided into three main groups. The first group are those estimated by recession analysis from observed flow data (for gauged catchments) or through regionalization for ungauged catchments (appendix 1), the second group are those estimated by model calibration

(for gauged catchments) against observed discharge or by regionalization methods (for ungauged catchments) (appendix 2), and the third group are those estimated from digitized geographic maps using a GIS (appendix 3). The snow routine in DDD has two parameters estimated from the spatial distribution of observed precipitation data (Skaugen and Weltzien, 2016). The shape parameter (a0) and the decorrelation length (d) of the gamma distribution of snow and snow water equivalent (SWE) are estimated from a previous calibration for 84 catchments in Norway (Skaugen et al., 2015). Since our study focuses on ungauged catchments, we cannot conduct calibration and recession analysis; therefore, we derived the model parameters needing calibration and recession analysis through combined method of regionalization using 41 gauged small rural catchments in Norway as a base (Tsegaw et al., 2019a). To estimate the regionalized parameters for this study (3 hourly time step), we have used the combined method of regionalization which has been recommended for estimating regionalized DDD model parameters with hourly resolution (Tsegaw et al., 2019a). In the combined method of regionalization, we have estimated the recession parameters and critical flux using multiple regression between model parameters and CDs, and the other parameters (all in appendix 2) using the physical similarity method with pooled donor catchments. The parameters of the model needing regionalization are shown in appendix 1 and 2 (the bottom 5 parameters in appendix 1 and all in appendix 2). The CDs of the study catchments, used for multiple regression, are presented in Table 1.

2.4 Impact study

We have extracted the precipitation and temperature data from the 4 X 4 km and 3 hourly resolution climate model. The climate data are forced into the DDD model to simulate the runoff, actual evapotranspiration and snow water equivalent (SWE) both for the reference and future

300 periods. We have used 30 hydrological years (1st of September to 31st of August) for both periods for the impact study. We have analyzed changes of the following climate impact indicators:

i) The mean annual changes of precipitation, temperature, flow, snow water equivalent (SWE) and actual evapotranspiration.

ii) The mean annual and mean seasonal changes of flow.

305 iii) The annual and seasonal flow duration curves (FDCs).

iv) The timing of annual winter/spring and fall stream flow.

v) The mean annual and seasonal maximum flows.

vi) Floods with return periods of 2 to 200 years

Changes are computed by Eq. (5) using the magnitudes of hydroclimatic variable for the reference

310 and future periods.

$$Change\ in\ x(\%) = \left(\frac{Future\ value\ of\ x - Reference\ value\ of\ x}{Reference\ value\ of\ x}\right) * 100 \qquad (5)$$

where x is any hydroclimatic variable.

2.4.1 Changes of hydroclimatic variables

315 The 3-hourly precipitation and temperature data, extracted from the climate model, are analyzed using an R-script to quantify the changes in the mean annual values for the reference and future periods. The 3-hourly precipitation data are aggregated yearly to estimate the annual precipitation value and then averaged over the 30 years to get the mean annual value. The 3-hourly temperature data are averaged for the whole 30 years to estimate the mean annual temperature. The simulated

320 3-hourly flow is averaged for the whole 30 years to get the mean annual flow data.

Seasonal mean flow data are also estimated for the reference and future periods i.e. winter, spring, summer and autumn for assessing changes in the seasonal mean flow. The annual maximum SWE is selected from each hydrological year and averaged for reference and future periods to get the mean annual maximum SWE for the two periods. The annual actual evapotranspiration is estimated by aggregating the actual evapotranspiration from the 3-hour simulation results and then averaged over 30 years to get the mean annual actual evapotranspiration.

2.4.2 Changes in flow duration curves

A flow duration curve is a cumulative curve that shows the percent of time a specified flow is equaled or exceeded during a given period, and it shows the flow characteristic of a stream throughout a range of flow, without regard to the sequence of occurrence (Searcy, 1959). We have analyzed changes in the stream flow variability over a water year between the reference and future periods. The changes of floods (between 0% and 10% exceedance), medium flows (between 10% and 70% exceedance) and low flows (between 70% and 100% exceedance) are analyzed in this study. The formula to calculate the probability of exceedance is given by Eq. (6).

$$p = 100 * {}^{K}/_{(n+1)} \quad (6)$$

p = the probability that a given flow will be equaled or exceeded (% of time).

K = the ranked position on the listing (dimensionless).

n = the number of events for period of record, and it is dimensionless.

2.4.3 Changes in timing of annual winter/spring and fall stream flow

The annual timing of river flows is a good indicator of climate-related changes. Changes in timing of annual winter/spring (WS) and fall stream flow are analyzed using center of volume date (Hodgkins et al., 2003). The center of volume date is the date by which half of the total volume of water for a given period flows by a river section. The center of volume date is expected to be more robust indicator of the timing of the bulk of high flows in a season than the peak flows, as the peak flow may happen before or after the bulk of seasonal flows (Hodgkins et al., 2003). From the 3-hour flow data (simulated for the reference and future periods), we have calculated the mean 3-hour flow for the 30 years in both periods. Using the mean 3-hour flow, we have computed seasonal center of volume dates for the winter/spring (1 January to 31 May) and fall (1 October to 31 December).

2.4.4 Changes in the maximum flows and flood frequency

The annual and seasonal maximum flows (floods) are selected from the 30 years of reference and future periods for the analysis. The changes in the mean and median of the annual and seasonal maximum flows are analyzed.

The number of 3-hour floods (frequency) above a certain threshold helps us to have a general overview on the impacts of climate change on the flood risk in small catchments. Accordingly, we have analyzed the changes in the number of 3-hour floods between the reference and future periods with a flow higher than the minimum of the 30 years annual maximum flow for the reference period.

To assess the magnitude of a flood with a given probability, flood frequency methods must be applied. Flood frequency analysis is important for flood hazard mapping, for which a flood of a certain return period (e.g. 200 years in Norway) is used for the flood zone mapping (Groen et al., 2012). To analyses changes in the magnitudes of a flood with a given return period (e.g. 200-year flood), flood frequency analysis is applied to the annual maximum series for the reference (1981 – 2011) and future periods (2070 – 2100). The percentage change in the flood magnitude is then computed as the difference between the two curves divided by the flood magnitude for the reference period. We have used a Gumbel distribution (Bhagat, 2017, Shaw, 1983) to model the annual maximum series in this study. We have selected the Gumbel distribution because it has been widely applied including the studies of climate change impacts on floods in Europe (Dankers and Feyen, 2008, Veijalainen et al., 2010).

3 Results

3.1 Regionalized DDD model parameters

The results of the parameters values from the regionalization for the six study catchments are presented in Table 3. The parameters and possible ranges of values are presented in appendix 4.

3.2 Changes in hydroclimatic variables

The simulation results of the hydrological model are further analyzed to quantify the changes in the hydroclimatic variables. The mean annual precipitation, the mean annual temperature, the mean annual evapotranspiration, the mean annual flow, the mean autumn flow, and the mean winter flow increase for all the study catchments in the future period compared to the reference period. The mean spring flow increases in the five catchments and decrease in one study

catchment. The mean summer flow decreases for the five catchments. The mean annual maximum SWE decreases for all the study catchments. In the future period, the mean annual precipitation increases by 20% to 24 %. The mean annual temperature rises in 3 - 3.3^{o}C. The mean annual flow increases from 17% to 33%. The decrease in the mean summer flow ranges from 7% to 35% and the increase is 4% in only one of the study catchments. The mean winter flow increases by an average of 127% (ranging from 41% to 256%). The mean spring flow increases by 4% to 100% for the five catchments and there will be a decrease by 1% in one catchment. The mean autumn flow increases by an average of 37% (ranging from 21% to 43%). The results of changes of the mean annual temperature, precipitation, maximum SWE and actual evapotranspiration are presented in Table 4. Table 5 presents changes in the mean annual and seasonal flows for the catchments. Mean 3-hourly flow of the study catchments are shown in Fig. 3 for the reference and future periods.

3.3 Changes in flow duration curves

The results of the study show that changes in the flow duration curves (FDCs) values are positive for all the flow conditions. The FDC values of the future period increase for all flow conditions (low, medium and high flows) for all the study catchments. For all catchments, the top 5% of flows in the future period are higher than the reference period by 8% to 62%. The median flow (flows which are exceeded by 50% of the time) increases by 24% to 140% (the highest value is for catchment 1 and the lowest value is for catchment 4) in the future period. Figure 4 shows the FDCs for both periods.

3.4 Changes in timing of annual winter/spring (WS) and fall stream flow

For all the study catchments, the mean WS center of volume dates occur earlier in the future period (16 - 68 days) than the reference period. The fall CV date occurs later for all the study catchments in the future period and a shift of 1 – 16 days is expected. Table 6 presents the mean WSCV dates and mean fall CV dates for all the study catchments.

3.5 Changes in the maximum flows and flood frequency

3.5.1 Changes in the annual and seasonal maximum flows

The annual and seasonal maximum flows increase in the future period compared to the reference period. The mean annual maximum flows increase from 29% to 38% across all the study catchments. The mean seasonal maximum flows also show an increase in all seasons (1 % to 118%) and all catchments except for spring season of catchment 2 (reduction of 29%) as shown in Table 7. The median of the annual and seasonal maximum flows increases for all catchments except for spring season of catchment 2 as shown in Fig.5. Table 7 presents the results of changes in the mean annual and seasonal maximum flows in future period compared to the reference period. Figure 5 shows the distributions of the 30 years annual and seasonal maximum flows both for the reference and future periods.

The number of 3-hours with floods exceeding the minimum annual maximum flood in the 30 years of the reference period increases in the future period significantly (Table 8). This result shows that

flooding will occur more often in the future period. In the future period, the yearly average number of such floods increase by 62% to 133% across all study catchments.

3.5.2 Changes in flood frequencies

The flood frequency analysis using Gumbel's Extreme Value Distribution shows that floods of 2, 5, 10, 20, 25, 50, 100 and 200 years return periods increase in the future period (2070 – 2100) compared to the reference period (1981 – 2011) for all catchments. The increase ranges from 16% to 43%. Table 9 shows the changes of flood frequencies for the selected return periods for all the study catchments.

4 Discussion

4.1 Regionalized DDD model parameters

The physical similarity assessment, between the study and gauged catchments in the west climate region of Norway, shows that the most similar gauged catchments are located close to the study catchments. The assessment result shows that the regionalization method used in this study is plausible.

4.2 Hydrological impacts of climate change

4.2.1 Changes of hydroclimatic variables

Generally, the findings of the increase in precipitation and temperature for the study catchments are in the range of increments predicted by the Norwegian Center for Climate Services (NCCS)

under the report Climate in Norway 2100 (Hanssen-Bauer et al., 2015) ; however, the results from some catchments are above or below the prediction interval of the report since the comparison is between catchments specific results with the regional values of the report. This is not unexpected since the comparison is between catchments specific values on a small scale and the regional values from the report. The NCCS report is based upon ten climate models with RCP8.5 and RCP4.5 using daily temporal resolution for the reference period (1971-2000) and future period (2071-2100).

The NCCS report shows that the median projections of change in the annual mean precipitation are 17% and 8% for RCP8.5 and RCP4.5 respectively, and projected increases in the mean annual temperature are by 3.7^{o}C to 2.3^{o}C for RCP8.5 and RCP4.5 respectively by 2100 for the south western part of Norway (where our study catchments are located). Our GCM-RCM-RCP8.5 result shows that the projected increase in the mean annual temperature is 3.3^{o}C and the mean annual precipitation change is 22% between 1981-2011 and 2070-2100 periods at the Bergen area of Norway. The comparison shows that the GCM-RCM-RCP8.5 climate model, used in this study, predicts slightly more precipitation than the NCCS report for RCP8.5 and colder than the NCCS report with RCP8.5.

In the future period, all the study catchments show an increase in the mean annual flow compared to the reference period. The minimum and maximum increases are 17% and 33% respectively. Alcamo et al. (2007) found that the mean annual river flow is projected to increase in northern Europe approximately by 9% to 22% up to 2070. This result aligns with our findings i.e. the

increment could increase by 17% to 33 % by 2100. The increase in mean annual flow in the future period is a result of a substantial increase in projected mean annual precipitation with a moderate increase in mean temperature i.e. the mean annual precipitation increases by 20% to 24% while the mean annual temperature increases by 3^{o}C to 3.3^{o}C (Table 4). The increase in the mean annual temperature results in an increase of water loss by evapotranspiration. However, the mean annual increase in precipitation exceeds the mean annual increase in the actual evapotranspiration computed in the model and these conditions contributed to increase of mean annual flow in general. The Hanssen-Bauer et al. (2015) report shows that the mean annual flow for western Norway (where the study catchments are located) could increase by -1% to 17% by 2100 and our result shows that the increase is slightly higher than the increase in the report for four of the study catchments. This may very well be related to the higher resolution of our regional climate model. The higher resolution enables, at least in theory, a better local representation of precipitation and temperature, and the averaging issue in estimating the regional value by the report may lead to differences.

Unlike the changes in the mean annual flow, changes in the temporal distribution of flows (e.g. seasonal) can be important because changes are rarely identical throughout the year (Olsson et al., 2016). The mean winter and autumn flows increase for all study catchments. The main causes of increases are projected increase in the precipitation and temperature during the autumn and winter seasons. The increase in mean winter flow contributes to much of the increase in the mean annual flow for all catchments (Table 5 and Fig.3). The main cause of increase in the mean winter flow is increased winter temperatures. Increased winter temperatures result in a higher proportion of winter precipitation to fall as rain which then results in a higher proportion of winter flow. The

mean spring flows show an increase for the five catchments and a decrease for one catchment while the mean summer flows show a decrease for the five catchments and an increase for one of the catchments. The increase in mean summer flow happened at a catchment which has the highest mean elevation (catchment 1 in table 1), and this result shows that the future increase in temperature may not result in high evapotranspiration to reduce the mean summer flows at the high elevation catchments.

Similar results are found in other hydrological assessments of the Bergen region. Previous studies of the water resources under climate change also project higher temperatures and increased annual precipitation in the Bergen region for the 2071-2100 future period under the RCP8.5 emissions scenario (Kristvik et al., 2018, Kristvik and Riisnes, 2015). Kristvik et al. (2018) based their assessment on statistical downscaling of an ensemble of RCPs and GCMs, followed by simulations of the hydrological response in term of inflow to surface water reservoirs. Due to higher temperatures and more rainfall precipitation, strong increases in winter flow was found, while a decrease was projected in spring/summer months due to less snowmelt (Kristvik et al. 2018).

The Hanssen-Bauer et al. (2015) report for western Norway shows that the mean winter and autumn flow increase by 15% to 42% and by 5% to 36% respectively by 2100. The findings of this study show that the increase in mean winter flow is higher than the maximum prediction reported by Hanssen-Bauer et al. (2015) for four catchments and to the higher end of the prediction in the report for the remaining two catchments. Similar results have been obtained for mean autumn flows except that three catchments have higher value than the maximum prediction value in the

report. The report predicts an increase of the mean spring flow by -9% to 17% and a decrease of mean summer flow by 13% to 28% by 2100. The findings of this study show that the increase in the mean spring flow is within the prediction interval of the report for three catchments and higher than the maximum prediction values of the report for the remaining three catchments. Wong et al. (2011) studied the differences in hydrological drought characteristics in summer season of Norway between the periods 1961-1990 and 2071-2100 using the HBV hydrological model with daily temporal resolution and found that substantial increases in hydrological drought duration and drought affected areas are expected in Norway which aligns with our findings. The Ministry of the Environment of Norway (2009) also pointed out that the summer flow in Norway is projected to be reduced and supports the findings of our study.

Climate change affects the snowpack and the amount of water stored in the snowpack (SWE). Increased winter temperature will generally lead to a reduction in snow storage and hence the mean maximum SWE will also be reduced in the future. The results of this study show that there will be a reduction in the mean maximum SWE at all the catchments in the future period. The reduction ranges from 48% to 78%. The largest reduction is found to be at the catchment with the highest mean elevation value (catchment 1). Snow accumulation and its characteristics are the results of air temperature, precipitation, wind and the amount of moisture in the atmosphere. Therefore, changes in these and other climatic properties can affect snowpack and hence maximum SWE. In our study, there is an increase temperature for all study catchments in the future period, and the increase resulted in the reduction of mean annual maximum SWE at all the study catchments.

4.2.2 Changes in flow duration curves (FDCs)

The results of this study show that climate change affects the FDCs of the study catchments. The future FDC is higher than the FDC of the reference period at all catchments for all probability of exceedances (Fig.4). The FDCs of all the study catchment show that the low flows increase in the future, and there will be longer periods with higher flows in the future period than in the reference period.

4.2.3 Changes in WSCV and fall CV dates

The mean winter/spring center of volume date (WSCV) will be earlier, and the mean fall CV date will be later for all the study catchments. The change in WSCV dates is related to the amount and timing of spring snowmelt and warmer winter temperature. The earlier mean WSCV date in the future period is the result of increased precipitation falling during a warmer winter, reduced snow storage, early snow melt and warmer spring temperature. The late occurrence of fall CV dates is related to the higher precipitation and temperature projected in fall in the future period. The warmer temperature in the future period makes the major proportion of future precipitation to happen as rain especially in the months of November and December which increases the future floods towards the end of a year and then the total flow volume in fall which makes the fall CV dates to occur later. The finding in our study is supported by the finding of Blöschl; G. et al (2017) i.e. in the southwestern part of Norway, there is a shift towards later floods due to climate change in the same period at the end of a year (October - December).

4.3 Changes in the maximum flows and flood frequency

4.3.1 Annual and seasonal maximum flows

In the future period (2070 – 2100), the results of this study show that there will be an increase in the mean and median of the annual and seasonal maximum flows (Table 7 and 8, and Fig.5) at all the study catchments except for the spring season of catchment 2. Most (15 – 23 of the 30 annual maximum floods) of the maximum annual flows happen during the autumn period (1st September to 30th of November) and therefore much of the contribution for the increment of the mean and median annual maximum flows comes from the autumn (Fig.5). The second largest contributor to the increment of the mean and median annual maximum flows is winter season (Fig.5). In the future period, the winter maximum flows increase in magnitude and frequencies as a substantial amount of precipitation falls as rain in a warmer climate. The mean summer maximum flows show the least increment in the future period (1% to 21%). The finding that mean annual maximum flows (floods) increase by 29% to 38% in our study is supported by Lawrence and Hisdal (2011). Lawrence and Hisdal (2011) have done ensemble modelling based on locally adjusted precipitation and temperature data from thirteen regional climate scenarios to assess likely changes in hydrological floods between a reference period (1960 – 1990) and two future periods (2021-2050) and (2071 - 2100), for the 115 catchments distributed throughout in Norway. Their results showed that western regions of Norway are associated with the largest percentage increases in the magnitude of the mean annual floods (> 20%). Lawrence and Hisdal (2011) also pointed out that increase in autumn and winter rainfall throughout Norway will increase the magnitude of peak flows during these seasons, and at areas already dominated by autumn and winter floods, the projected increases in floods magnitude will be large. Since our study catchments are at western Norway which is dominated by autumn floods and our finding (Fig.5) confirms their finding in

that the maximum increases in floods magnitude are expected to happen in autumn and winter seasons (Table 7 and Fig.5).

The yearly average number of 3-hours flows, which are greater than the minimum of the annual maximum high flows in the 30 years of the reference period increases. The yearly average number of such floods increase between 61.7% and 133% across all study catchments as presented in Table 8. The results show that there will be a greater number of 3-hours floods in the future period than the reference period, and more flood risks are expected at the infrastructures constructed downstream of small ungauged rural catchments in west coast Norway near Bergen city. European Environmental Agency(2004b), in: Alcamo et al. (2007) found that the risk of floods increases in northern Europe (e.g. Norway) which supports our finding of increase in the risk of floods. Center for International Climate Research (https://cicero.oslo.no) predicts that western Norway will experience more heavy rain and flooding in the future and our findings confirms their predictions.

4.3.2 Changes in flood frequency

The study results from the six ungauged small catchments show that there will be an increase in flood frequencies with a return periods of 2, 5, 10, 20, 25, 50, 100, 200 years in the future period. The changes of all return periods for all catchments are in between 16% and 43%. The maximum and the minimum changes happen for a return period of 200 years. For all return periods, the mean changes are between 31 % and 32% while the median changes are between 30% and 34%. The 2, 5, 10 years changes are greater than 20% for all catchments, and 20, 25, 50, 100 and 200-years changes are greater than 20% for five of the six study catchments.

Beldring et al. (2006) studied the percentage change in the mean annual flood and the 50-year flood in four catchments in Norway between 1961-1990 and 2070-2100 in which one of the catchments is in western Norway (Viksvatn in Gaular) and found that moderate to large increases are expected. Their result is supported by our finding i.e. the 50-year flood on six small catchments in west Norway will increase by 18% to 40 % between 1981 -2011 and 2070-2100. The results of our study show that the 200-year flood changes range from 16% to 43% for the study catchments. Lawrence and Hisdal (2011) have found that the projected increase of the 200-year flood exceed 40% for some of the catchments in western Norway between the 1961-1990 reference period and the 2071- 2100 future period which is in agreement with our findings. Lawrence (2016) used ensembles of regional climate projections from EURO-CORDEX together with HBV model to assess possible effects of climate change on floods on 115 catchments in Norway for two future periods (2031-2060 and 2071-2100). The assessment result shows that the minimum increase in the 200 years flood for catchments less than 100km^2 at Hordaland county (where the study catchments are located) is 20% which is generally in agreement with our findings.

Lawrence (2016) showed that the increase in the 200 years flood is higher for RCP8.5 than RCP 4.5 in Hordaland county. Not surprising that the choice of RCP has significant effect on the results of the 200years flood frequency. Of the 115 catchments used in the study for the whole Norway, 10 of them are in the Hordaland county. With emission scenario RCP4.5, eight of the ten catchments showed less than 20 % increase (1 catchment a decrease, 2 catchments an increase between 1% - 10%, 5 catchments an increase between 11% - 20%), and two catchments show an increase greater than 20% (1 catchment an increase between 21% - 30% and 1 catchment an

increase between 31% - 40%. With emission scenario RCP8.5, seven of the ten catchments show greater than 20 % increase (3 catchments an increase between 21% - 30% and 4 catchments an increase between 31% - 40%), and 3 catchments show an increase of less than 20% (1 catchment a decrease and 2 catchments an increase between 11% - 20%). The result of our study shows that the 200-year flood changes range from 16% to 43% (1 catchment between 10% -20%, 1 catchment between 20% -30%, 2 catchments between 30% - 40% and 2 catchments between 40% and 50%). Generally, our finding with RCP8.5 is similar to the Lawrence (2016) finding with RCP8.5 except that our finding shows an increase greater than 40% for some study catchments.

The main differences between our study and the study of Lawrence (2016) are the number and types of climate models, RCPs, the catchment sizes and the temporal resolution. The comparisons of the increase in flood risks are mainly done in the same county (Hordaland county where Bergen area is located) and the area is mainly dominated by floods generated by rain in autumn season. However, in the Lawrence (2016) study the catchment sizes are ranging from 6km^2 to 15449km^2 and used 10 global-regional models with RCP8.5 and RCP4.5. The temporal resolution used in the Lawrence (2016) study is daily and perhaps this is the data which has been bias corrected after the GCM-RCM chain. Changes above 41% for some catchments in our findings are related with the differences in the climate models, differences in the bias correction method, difference in the temporal resolutions used, difference in the hydrological models used, differences in the sizes of the catchments and capability of the DDD model in predicting 3 hourly floods in small catchments. Our findings are based on RCP8.5 scenario which can be used as a worst-case scenario at the Bergen area in the south western part of Norway.

4.4 Limitations

There are limitations in this study which are related to DDD model and the climate model. A first limitation is related to the DDD model parameters. In this study, we have used the regionalization of DDD model parameters developed for 1 hour (Tsegaw et al., 2019a) to estimate parameters for the 3-hour simulation. DDD model parameters like degree hour factor for evapotranspiration (Cea) and degree hour factors for snow melt (Cx) can be sensitive to the temporal resolution. However, the same uncertainty is present both in the reference and future period. The second limitation is related to the simple degree evaporation model used in the DDD. Table 4 shows big changes in actual evapotranspiration, and the big change in actual evapotranspiration tells us that in the future period there will be higher water available (to evaporate) and higher temperature (to cause evaporation) than the reference period; however, there is a limitation with the simple evaporation model since actual evaporation is not only affected by temperature but by additional climatological factors like wind speed, humidity, cloudiness etc. This limitation could also be the reason for a big change of actual evapotranspiration between the reference (1981-2011) and future period (1970-2100). A third possible limitation is that the DDD model parameters are assumed to be constant under changing climatic conditions, and the same parameter sets are used for the reference and future period simulations. However, studies show that using the same parameter sets for the reference and future periods under climate impact studies can have significant impact on the simulation results (Merz et al. (2011). A fourth limitation is that the modelled changes in the hydroclimatic variables and flood frequency are derived from a single GCM-RCM model chain using only the RCP8.5 scenario. Thereby, we are not able to capture the GCM-RCM uncertainties usually found by handling model ensembles. However, this simulation has the benefit of a high spatial resolution for a better representation of small-scale features and additionally a novel bias

correction method has been applied prior to the downscaling to ensure physical consistency between temperature and precipitation variables used as input to the hydrological model.

675

We present one realization of a climate scenario, and that we recommend applying the method of Pontoppidan (2018) to other GCMs to capture model uncertainties. Further, the comparison done between our study and other studies shows that we are not totally off, and that the findings can give a useful addition to the current understandings of the effects of changing climate on the west
680 coast. Other combinations of GCMs-RCMs-RCPs predict varieties of future climate change signals which could potentially result in different hydroclimatic and flood predictions for the same study catchments. Therefore, the results of this study alone should not be taken as a conclusive of what will be seen in the future but could be of practical use to regional decision-makers if considered alongside other previous and future findings.

685

5 Conclusion

In this study we use a newly developed bias corrected dynamical downscaling product as input for the DDD model to investigate the impact of climate change on small ungauged catchments in western Norway. The results show that there will be an increase in the mean annual flow in the
690 future period. The increase in the mean annual flow is due to the increase in the mean autumn, winter and spring flows in the future period (2070-2100) compared to the reference period (1981 - 2011). In the future period, the mean summer flows from the study catchments decrease. Future flow duration curves are higher than the flow duration curves of the reference period for all study catchments for all probability of exceedances. The median flow (flows which are exceeded by

695 50% of the time) increases by 24% to 140%. The FDCs of all the study catchment show that the low flows increase in the future, and there will be more wetter periods in the future than in the reference period.

There will be an increase in the mean annual floods and flood frequencies of 2, 5, 10, 20, 25, 50,
700 100 and 200 years in the future period. The mean annual maximum floods increase by 29% to 38%. This study gives clear indication that the projected increase in flood frequencies are high (e.g. 200-year flood > 40%) in small catchments around Berge area of western Norway, and such catchments are vulnerable to an increased risk in the future climate. The high-resolution regional climate model with a novel bias correction method improves the knowledge and understanding of
705 climate change impacts on hydrology of small catchments in western Norway. However, it is important to conduct further research which can address the limitations of this study before conducting flood risk assessment and planning flood risk management strategies as a national strategy for climate change adaptation.

710 These simulations are based on high resolution regional climate model projection with a novel bias correction method and address limitations in previous impact studies where such projections have not yet been available and enabling in-depth analysis of the impacts of climate change on rapid hydrological processes. An ensemble of GCM-RCM runs building on the results of this paper is suggested as a venue for further work in order to account for uncertainties in future emissions and
715 climate projections and thus provide more reliable recommendations for infrastructure design and adaptation.

Acknowledgments

The authors would like to acknowledge Norwegian Climate Service Centre for providing information on how to access and process the 3 X 3 km spatial and 3-hours temporal resolution gridded precipitation and temperature climate data for western Norway. The authors also would like to acknowledge Thomas Skaugen of the Norwegian Water Resources and Energy Directorate (NVE) for providing the source code of the Distance Distribution Dynamics hydrological model. Finally, the authors gratefully acknowledge the financial support by Bingo and ExtndBingo project (EU Horizon 2020, grant agreement 641739), and the Research Council of Norway (RCN) through R3 (grant 255397) and through the Centre for Research-based Innovation "Klima 2050" (see www.klima2050.no). We also would like to thank UNINETT Sigma2 because the regional downscaling was performed on resources provided by UNINETT Sigma2 - the National Infrastructure for High Performance Computing and Data Storage in Norway.

References

Alcamo, J., FlÖRke, M., and MÄRker, M.: Future long-term changes in global water resources driven by socio-economic and climatic changes, Hydrological Sciences Journal, 52, 247-275, https://doi.org/210.1623/hysj.1652.1622.1247, 2007.

Alfieri, L., Burek, P., Feyen, L., and Forzieri, G.: Global warming increases the frequency of river floods in Europe, Hydrol. Earth Syst. Sci., 19, 2247-2260, https://doi.org/2210.5194/hess-2219-2247-2015, 2015.

Azad, R. and Sorteberg, A.: Extreme daily precipitation in coastal western Norway and the link to atmospheric rivers, Journal of Geophysical Research: Atmospheres, 122, 2080-2095, https://doi.org/2010.1002/2016JD025615, 2017.

Baltas, E. A.: Impact of Climate Change on the Hydrological Regime and Water Resources in the Basin of Siatista, International Journal of Water Resources Development, 23, 501-518, https://doi.org/510.1080/07900620701485980, 2007.

Beldring, S., Roald, L. A., Engen-Skaugen, T., and Førland, E. J.: Climate Change Impacts on Hydrological Processes in Norway 2071-2100. Based on RegClim HIRHAM and Rossby Centre RCAO Regional Climate Model Results. Norwegian Water Resources and Energy Directorate, Oslo, Norway, 2006.

Bhagat, N.: Flood Frequency Analysis Using Gumbel's Distribution Method: A Case Study of Lower Mahi Basin, India, Ocean Development and International Law, 6, 51-54, https://doi.org/10.11648/j.wros.20170604.20170611, 2017.

Blöschl; G. et al. Changing climate shifts timing of European floods. Science, 357, 588-590, https://doi.org/10.1126/science.aan2506, 2017.

Blöschl, G., Hall, J., Viglione, A. *et al.* Changing climate both increases and decreases European river floods. *Nature* **573,** 108–111, https://doi.org/10.1038/s41586-019-1495-6, 2019.

Borga, M., Anagnostou, E. N., Blöschl, G., and Creutin, J. D.: Flash flood forecasting, warning and risk management: the HYDRATE project, Environmental Science and Policy, 14, 834-844, https://doi.org/810.1016/j.envsci.2011.1005.1017, 2011.

Bras, R. L.: Hydrology: An Introduction to Hydrologic Science, Addison-Wesley, 1990.

Bruyère, C.L., Done, J.M., Holland, G.J. *et al.* Bias corrections of global models for regional climate simulations of high-impact weather. *Clim Dyn* **43,** 1847–1856. https://doi.org/10.1007/s00382-013-2011-6, 2014.

Chernet, H. H., Alfredsen, K., and Midttømme, G. H.: Safety of Hydropower Dams in a Changing Climate, Journal of Hydrologic Engineering, 19, 569-582, https://doi.org/510.1061/(ASCE)HE.1943-5584.0000836, 2014.

Christensen, J. H., Boberg, F., Christensen, O. B., and Lucas-Picher, P., On the need for bias correction of regional climate change projections of temperature and precipitation, *Geophys. Res. Lett.*, 35, L20709, doi:10.1029/2008GL035694. 2008.

Dankers, R. and Feyen, L.: Climate Change Impact on Flood Hazard in Europe: An Assessment Based on High-Resolution Climate Simulations, Journal of Geophysical Research, 113, D19105, https://doi.org/19110.11029/12007JD009719, 2008.

Dee, D.P., Uppala, S.M., Simmons, A.J., Berrisford, P., Poli, P., Kobayashi, S., Andrae, U., Balmaseda, M.A., Balsamo, G., Bauer, P., Bechtold, P., Beljaars, A.C.M., van de Berg, L., Bidlot, J., Bormann, N., Delsol, C., Dragani, R., Fuentes, M., Geer, A.J., Haimberger, L., Healy, S.B., Hersbach, H., Hólm, E.V., Isaksen, L., Kållberg, P., Köhler, M., Matricardi, M., McNally, A.P., Monge-Sanz, B.M., Morcrette, J.-J., Park, B.-K., Peubey, C., de Rosnay, P., Tavolato, C., Thépaut, J.-N. and Vitart, F., The ERA-Interim reanalysis: configuration and performance of the data assimilation system. Q.J.R. Meteorol. Soc., 137: 553-597. doi:10.1002/qj.828, 2011.

Donnelly, C., Greuell, W., Andersson, J., Gerten, D., Pisacane, G., Roudier, P., and Ludwig, F.: Impacts of climate change on European hydrology at 1.5, 2 and 3 degrees mean global warming above preindustrial level, Climatic Change, 143, 13-26, http://dx.doi.org/10.1007/s10584-10017-12022-10580., 2017.

Eisenreich, S., Bernasconi, C., and Campostrini, P.: Climate change and the European water dimension, 2005.

Fleig, A. K. and Wilson, D.: Flood estimation in small catchments : literature study. In: Naturfareprosjektet,, Rapport (Norges vassdrags- og energidirektorat : online), Norwegian Water Resources and Energy Directorate, Oslo, 2013.

Golz, S., Naumann, T., Neubert, M., and Günther, B.: Heavy rainfall: An underestimated environmental risk for buildings?, E3S Web of Conferences, 7, 08001, https://doi.org/08010.01051/e08003sconf/20160708001, 2016.

Groen, R., M. Jespersen, K. de Jong, and Olsson, J.: Climate change impacts and uncertainties in flood risk management: Examples from the North Sea Region. Norwegian Water Resources and Energy Directorate Oslo, 2012.

Hanssen-Bauer, I., E.J. Førland, I. Haddeland, H. Hisdal, S. Mayer, A. Nesje, J.E.Ø. Nilsen, S. Sandven, A.B. Sandø, and Ådlandsvik, A. S. o. B.: KLIMA I NORGE 2100. Miljø Direktoratet,Oslo, 2015.

Hattermann, F., Kundzewicz, Z., Becker, C., Castelletti, A., Gooch, G., Kaden, S., de Lange, W., Laurans, Y., Muhar, S., Pahl-Wostl, C., Soncini-Sessa, R., Stålnacke, P., and Willems, P.: Water Framework Directive: Model supported Implementation. A Water Manager's Guide, 2009.

Hodgkins, G. A., Dudley, R., and Huntington, T.: Changes in the Timing of High River Flows in New England Over the 20th Century, 2003.

IPCC: Summary for Policymakers. In: Global Warming of 1.5°C. An IPCC Special Report on the impacts of global warming of 1.5°C above pre-industrial levels and related global greenhouse gas emission pathways, in the context of strengthening the global response to the threat of climate change, sustainable development, and efforts to eradicate poverty [Masson-Delmotte, V., P. Zhai, H.-O. Pörtner, D. Roberts, J. Skea, P.R. Shukla, A. Pirani, W. Moufouma-Okia, C. Péan, R. Pidcock, S. Connors, J.B.R. Matthews, Y. Chen, X. Zhou, M.I. Gomis, E. Lonnoy,T. Maycock, M. Tignor, and T. Waterfield (eds.)] World Meteorological Organization, Geneva, Switzerland, 32 pp., **2018**.

Jacob, D., Petersen, J., Eggert, B., Alias, A., Christensen, O. B., Bouwer, L. M., Braun, A., Colette, A., Déqué, M., Georgievski, G., Georgopoulou, E., Gobiet, A., Menut, L., Nikulin, G., Haensler, A., Hempelmann, N., Jones, C., Keuler, K., Kovats, S., Kröner, N., Kotlarski, S., Kriegsmann, A., Martin, E., van Meijgaard, E., Moseley, C., Pfeifer, S., Preuschmann, S., Radermacher, C., Radtke, K., Rechid, D., Rounsevell, M., Samuelsson, P., Somot, S., Soussana, J.-F., Teichmann, C., Valentini, R., Vautard, R., Weber, B., and Yiou, P.: EURO-CORDEX: new high-resolution climate change projections for European impact research, Regional Environmental Change, 14, 563-578, http://dx.doi.org/510.1007/s10113-10014-10587-y., 2014.

Kim, E. S. and Choi, H. I.: Estimation of the relative severity of floods in small ungauged catchments for preliminary observations on flash flood preparedness: a case study in Korea, Int J Environ Res Public Health, 9, 1507-1522, https://doi.org/1510.3390/ijerph9041507, 2012.

Kotlarski, S., Keuler, K., Christensen, O. B., Colette, A., Déqué, M., Gobiet, A., Goergen, K., Jacob, D., Lüthi, D., van Meijgaard, E., Nikulin, G., Schär, C., Teichmann, C., Vautard, R., Warrach-Sagi, K., and Wulfmeyer, V.: Regional climate modeling on European scales: a joint standard evaluation of the EURO-CORDEX RCM ensemble, Geosci. Model Dev., 7, 1297-1333, https://doi.org/1210.5194/gmd-1297-1297-2014, 2014.

Kristvik, E., Muthanna, T. M., and Alfredsen, K.: Assessment of future water availability under climate change, considering scenarios for population growth and ageing infrastructure, Journal of Water and Climate Change, 10, 1-12, https://doi.org/10.2166/wcc.2018.2096, 2018.

Kristvik, E., & Riisnes, B., *Hydrological Assessment of Water Resources in Bergen.* Masters thesis, Norwegian University of Science and Technoloy, Trøndheim, Norway, 2015

Krysanova, V., Vetter, T., and Hattermann, F.: Detection of change in drought frequency in the Elbe basin: comparison of three methods, Hydrological Sciences Journal, 53, 519-537, https://doi.org/510.1623/hysj.1653.1623.1519, 2008.

Kundzewicz, Z. W., Kanae, S., Seneviratne, S. I., Handmer, J., Nicholls, N., Peduzzi, P., Mechler, R., Bouwer, L. M., Arnell, N., Mach, K., Muir-Wood, R., Brakenridge, G. R., Kron, W., Benito, G., Honda, Y., Takahashi, K., and Sherstyukov, B.: Flood risk and climate change: global and regional perspectives, Hydrological Sciences Journal, 59, 1-28, https://doi.org/10.1080/02626667.02622013.02857411, 2014.

Lawrence, D.: Klimaendring og framtidige flommer i Norge. avdeling, H. (Ed.), Norges vassdrags- og energidirektorat, Oslo, 2016.

Lawrence, D. and Hisdal, H.: Hydrological projections for floods in Norway under a future climate, Norwegian Water Resources and Energy Directorate, Oslo, 2011.

Lespinas, F., Ludwig, W., and Heussner, S.: Hydrological and climatic uncertainties associated with modeling the impact of climate change on water resources of small Mediterranean coastal rivers, Journal of Hydrology, 511, 403–422, https://doi.org/410.1016/j.jhydrol.2014.1001.1033, 2014.

Li, Z.: Watershed modeling using arc hydro based on DEMs: a case study in Jackpine watershed, Environmental Systems Research, 3, 1-11, https://doi.org/10.1186/2193-2697-1183-1111, 2014.

López-Moreno, J. I., Pomeroy, J. W., Revuelto, J., and Vicente-Serrano, S. M.: Response of snow processes to climate change: spatial variability in a small basin in the Spanish Pyrenees, Hydrological Processes, 27, 2637-2650, https://doi.org/2610.1002/hyp.9408, 2013.

Madsen, H., Lawrence, D., Lang, M., Martinkova, M., and Kjeldsen, T. R.: Review of trend analysis and climate change projections of extreme precipitation and floods in Europe, Journal of Hydrology, 519, 3634-3650, https://doi.org/3610.1016/j.jhydrol.2014.3611.3003, 2014.

Mallakpour, I. and Villarini, G.: The changing nature of flooding across the central United States, Nature Climate Change, 5, 250-254, https://doi.org/210.1038/nclimate2516, 2015.

Maraun, D. Bias Correcting Climate Change Simulations - a Critical Review. *Curr Clim Change Rep* 2**,** 211–220. https://doi.org/10.1007/s40641-016-0050-x, 2016.

Maraun, D., Shepherd, T., Widmann, M. *et al.* Towards process-informed bias correction of climate change simulations. *Nature Clim Change* 7**,** 764–773 https://doi.org/10.1038/nclimate3418, 2017.

Menzel, L., Niehoff, D., Bürger, G., and Bronstert, A.: Climate change impacts on river flooding: A modelling study of three meso-scale catchments, Climatic Change: Implications for the Hydrological Cycle and for Water Management,, 10, 249-269, https://doi.org/210.1007/1000-1306-47983-47984_47914 2006.

Merz, R., Parajka, J., and Blöschl, G.: Time stability of catchment model parameters: Implications for climate impact analyses, Water Resources Research - WATER RESOUR RES, 47, W02531, https://doi.org/02510.01029/02010WR009505, 2011.

Ministry of the Environment of Norway: Norway's Fifth National Report under the United Nation's Framework Convention on Climate Change. 2009.

Muerth, M. J., Gauvin St-Denis, B., Ricard, S., Velázquez, J. A., Schmid, J., Minville, M., Caya, D., Chaumont, D., Ludwig, R., and Turcotte, R.: On the need for bias correction in regional climate scenarios to assess climate change impacts on river runoff, Hydrol. Earth Syst. Sci., 17, 1189–1204, https://doi.org/10.5194/hess-17-1189-2013, 2013.

Olsson, J., Arheimer, B., Borris, M., Donnelly, C., Foster, K., Nikulin, G., Persson, M., Perttu, A.-M., Uvo, C. B., Viklander, M., and Yang, W.: Hydrological Climate Change Impact Assessment at Small and Large Scales: Key Messages from Recent Progress in Sweden, Climate, 4, 39, https://doi.org/10.3390/cli4030039, 2016.

Pontoppidan, M., Kolstad, E. W., Sobolowski, S., and King, M. P.: Improving the Reliability and Added Value of Dynamical Downscaling via Correction of Large-Scale Errors: A Norwegian Perspective, Journal of Geophysical Research: Atmospheres, 123, 11,875-811, 888, https://doi.org/810.1029/2018JD028372, 2018.

Pontoppidan, M., Reuder, J., Mayer, S., and Kolstad, E. W.: Downscaling an intense precipitation event in complex terrain: the importance of high grid resolution, Tellus A: Dynamic Meteorology and Oceanography, 69, 1271561, https://doi.org/1271510.1271080/16000870.16002016.11271561, 2017.

Pumo, D., Caracciolo, D., Viola, F., and Noto, L. V.: Climate change effects on the hydrological regime of small non-perennial river basins, Science of The Total Environment, 542, 76-92, https://doi.org/10.1016/j.scitotenv.2015.1010.1109, 2016.

Quintero, F., Mantilla, R., Anderson, C., Claman, D., and Krajewski, W.: Assessment of Changes in Flood Frequency Due to the Effects of Climate Change: Implications for Engineering Design, Hydrology, 5, 1-19, https://doi.org/10.3390/hydrology5010019, 2018.

Rasmussen, R., C. Liu, K. Ikeda, D. Gochis, D. Yates, F. Chen, M. Tewari, M. Barlage, J. Dudhia, W. Yu, K. Miller, K. Arsenault, V. Grubišić, G. Thompson, and E. Gutmann.: High-Resolution Coupled Climate Runoff Simulations of Seasonal Snowfall over Colorado: A Process Study of Current and Warmer Climate. *J. Climate*, 24, 3015–3048, https://doi.org/10.1175/2010JCLI3985.1, 2011.

Richardson, D.: Flood risk—the impact of climate change, Proceedings of the Institution of Civil Engineers - Civil Engineering, 150, 22-24, https://doi.org/10.1680/cien.2002.1150.1685.1622, 2002.

Roald, L.A., Rainfall floods and weather patterns. Report, Norwegian Water Resources and Energy Directorate, Oslo, Norway, 2008.

Rocheta, E., J.P. Evans, and Sharma, A., Can Bias Correction of Regional Climate Model Lateral Boundary Conditions Improve Low-Frequency Rainfall Variability?. *J. Climate*, 30, 9785–9806, https://doi.org/10.1175/JCLI-D-16-0654.1, 2017.

Rojas, R., Feyen, L., and Watkiss, P.: Climate change and river floods in the European Union: Socio-economic consequences and the costs and benefits of adaptation, Global Environmental Change, 23, 1737-1751, https://doi.org/1710.1016/j.gloenvcha.2013.1708.1006, 2013.

Schär , C., Frei, C., Lüthi, D., and Davies, C., Surrogate climate-change scenarios for regional climate models. *Geophysical Research Letters*, *23*(6), 669 - 672. https://doi.org/10.1029/96GL00265, 1996.

Searcy, J.: Flow-Duration Curves, 1959.

Skamarock, W. C., Klemp, J., Dudhia, J., Gill, D. O., Barker, D., and Wang, W.: A Description of the Advanced Research WRF Version 3, University Corporation for Atmospheric Research. , 27, 3-27, https://doi.org/10.5065/D5068S5064MVH, 2008.

Skaugen, T. and Mengistu, Z.: Estimating catchment-scale groundwater dynamics from recession analysis – enhanced constraining of hydrological models, Hydrol. Earth Syst. Sci., 20, 4963-4981, https://doi.org/4910.5194/hess-4920-4963-2016, 2016.

Skaugen, T. and Onof, C.: A rainfall-runoff model parameterized from GIS and runoff data, Hydrological Processes, 28, 4529-4542, https://doi.org/4510.1002/hyp.9968, 2014.

Skaugen, T., Peerebom, I. O., and Nilsson, A.: Use of a parsimonious rainfall–run-off model for predicting hydrological response in ungauged basins, Hydrological Processes, 29, 1999-2013, https://doi.org/1910.1002/hyp.10315, 2015.

Skaugen, T. and Weltzien, I. H.: A model for the spatial distribution of snow water equivalent parameterized from the spatial variability of precipitation, The Cryosphere, 10, 1947-1963, https://doi.org/1910.5194/tc-1910-1947-2016, 2016.

Thornes, J. E.: IPCC, 2001: Climate change 2001: impacts, adaptation and vulnerability, Contribution of Working Group II to the Third Assessment Report of the Intergovernmental Panel on Climate Change, edited by J. J. McCarthy, O. F. Canziani, N. A. Leary, D. J. Dokken and K. S. White (eds). Cambridge University Press, Cambridge, UK, and New York, USA, 2001, ISBN 0-521-01500-6 (paperback), ISBN 0-521-80768-9 (hardback), International Journal of Climatology, 22, 1285-1286, https://doi.org/1210.1002/joc.1775, 2002.

Tofiq, F. A. and Guven, A.: Prediction of design flood discharge by statistical downscaling and General Circulation Models, Journal of Hydrology, 517, 1145-1153, https://doi.org/1110.1016/j.jhydrol.2014.1106.1028 2014.

Tramblay, Y., Ruelland, D., Somot, S., Bouaicha, R., and Servat, E.: High-resolution Med-CORDEX regional climate model simulations for hydrological impact studies: a first evaluation of the ALADIN-Climate model in Morocco, Hydrol. Earth Syst. Sci., 17, 3721–3739, https://doi.org/10.5194/hess-17-3721-2013, 2013

Tsegaw, A. T., Alfredsen, K., Skaugen, T., and Muthanna, T. M.: Predicting hourly flows at ungauged small rural catchments using a parsimonious hydrological model, Journal of Hydrology, 573, 855-871, https://doi.org/810.1016/j.jhydrol.2019.1003.1090, 2019a.

Tsegaw, A. T., Skaugen, T., Alfredsen, K., and Muthanna, T. M.: A dynamic river network method for the prediction of floods using a parsimonious rainfall-runoff model, Hydrology Research, 2019b. https://doi.org/10.2166/nh.2019.2003, 2019b.

Vannitsem, S.: Bias correction and post-processing under climate change, Nonlin. Processes Geophys., 18, 911–924, https://doi.org/10.5194/npg-18-911-2011, 2011.

Veijalainen, N., Lotsari, E., Alho, P., Vehviläinen, B., and Käyhkö, J.: National Scale Assessment of Climate Change Impacts on Flooding in Finland, Journal of Hydrology, 391, 333-350, https://doi.org/310.1016/j.jhydrol.2010.1007.1035, 2010.

Vormoor, K., Lawrence, D., Heistermann, M., and Bronstert, A.: Climate change impacts on the seasonality and generation processes of floods – projections and uncertainties for catchments with mixed snowmelt/rainfall regimes, Hydrology and earth System Sciences, 19, 913–931, https://www.doi:10.5194/hess-19-913-2015, 2015.

Wang, J. and Kotamarthi, V.R., High-resolution dynamically downscaled projections of precipitation in the mid and late 21st century over North America. Earth's Future, 3: 268-288. doi:10.1002/2015EF000304, 2015.

Wong, W. K., Beldring, S., Engen-Skaugen, T., Haddeland, I., and Hisdal, H.: Climate Change Effects on Spatiotemporal Patterns of Hydroclimatological Summer Droughts in Norway, Journal of Hydrometeorology, 12, 1205-1220, https://www.jstor.org/stable/24912722, 2011.

Xu, Z. and Yang Z., : An Improved Dynamical Downscaling Method with GCM Bias Corrections and Its Validation with 30 Years of Climate Simulations. *J. Climate,* **25**, 6271–6286, https://doi.org/10.1175/JCLI-D-12-00005.1, 2012.

Xu, Z, and Yang, Z-L, A new dynamical downscaling approach with GCM bias corrections and spectral nudging. *J. Geophys. Res. Atmos.*, 120, 3063– 3084. doi: 10.1002/2014JD022958, 2015.

Zappa, G., Shaffrey, L., and Hodges, K.: The Ability of CMIP5 Models to Simulate North Atlantic Extratropical Cyclones*, Journal of Climate, 26, 5379-5396, https://doi.org/5310.1175/JCLI-D-5312-00501.00501, 2013.

Appendixes

Appendix 1. List of DDD model parameters estimated from observed precipitation data and those estimated from regionalization (multiple regression) for the study catchments.

Parameters	Description of the parameter	Method of estimation	Unit
d	Parameter for spatial distribution of SWE, decorrelation length	From spatial distribution of observed precipitation	Positive real number
a0	Parameter for spatial distribution of SWE, shape parameter	From spatial distribution of observed precipitation	Positive real number
MAD	Long term mean annual discharge	Specific runoff map of Norway	$m^3 sec^{-1}$
Gshape	Shape parameter of λ	Regression	Positive real number
Gscale	Scale parameter of λ	Regression	Positive real number
GshInt	Shape parameter of Λ	Regression	Positive real number
GscInt	Scale parameter of Λ	Regression	Positive real number
Fc	Critical flux	Regression	m^3/hour

Appendix 2. List of DDD rainfall-runoff model parameters estimated from pooling group of physical similarity method of regionalizations.

Parameters	Description of the parameter	Method of estimation	Unit
Pro	Liquid water in snow	Regionalization (poolig group)	fraction
Cx	Degree hour factor for snow melt	Regionalization (poolig group)	mm $^{o}C^{-1}$ $hour^{-1}$
CFR	Degree hour factor for refreezing	Regionalization (poolig group)	mm $^{o}C^{-1}$ $hour^{-1}$
Cea	Degree hour factor for evapotranspiration	Regionalization (poolig group)	mm $^{o}C^{-1}$ $hour^{-1}$
rv	Celerity for river flow	Regionalization (poolig group)	m/s

Appendix 3. List of DDD rainfall-runoff model parameters estimated from geographical data using GIS.

Symbol of parameters	Description of the Parameter
area	Catchment area
maxLbog	Maximum distance of marsh land portion of hillslope
midLbog	Mean distance of marsh land portion of hillslope
bogfrac	Areal fraction of marsh land from the total land uses
zsoil	Areal fraction of DD for soils (what area with distance zero to the river)
zbog	Areal fraction of distance distribution for marsh land (what area with distance zero to the river)
midFl	Mean distance (from distance distribution) for river network
stdFL	Standard deviation of distance (from distance distribution) for river network
maxFL	Maximum distance (from distance distribution) for river network
maxDl	Maximum distance (from distance distribution) of non-marsh land (soils) of hill slope
midDL	Mean distance (from distance distribution) of non-marsh land (soils) of hill slope
midGl	Mean distance (from distance distribution) for Glacial
stdGl	Standard deviation of distance (from distance distribution) for Glacial
maxGl	Maximum distance (from distance distribution) for Glacial
Hypsographic curve	11 values describing the quantiles 0, 10, 20, 30, 40, 50, 60,70,80,90,100

Appendix 4. Possible ranges of regionalized DDD model parameters

Model parameters needing regionalization	Method of regionalization	Possible ranges of values
Gshape	Multiple regression	Positive real number
Gscale	Multiple regression	Positive real number
GshInt	Multiple regression	Positive real number
GscInt	Multiple regression	Positive real number
fc	Multiple regression	Positive real number
Pro	Pooling group type of physical similarity	0.03 - 0.1
Cx	Pooling group type of physical similarity	0.05 - 1.0
CFR	Pooling group type of physical similarity	0.001 - 0.01
Cea	Pooling group type of physical similarity	0.01 - 0.1
rv	Pooling group type of physical similarity	0.5 - 1.5

1055

Figure Captions

Figure 1. Locations of study catchments in Norway

Figure 2. Structure of the Distance Distributions Dynamics model adapted from Skaugen and Onof (2014). Left panel: the storage model and right panel: hydrographs of hillslope and river. P is precipitation, T is temperature, E is actual evapotranspiration, G(t) is input from snowmelt and rain, Z(t) is soil moisture in unsaturated zone, X(t) is excess water, M is total volume of subsurface water reservoir, S(t) a saturated zone volume and D (t) is unsaturated zone volume.

Figure 3. Yearly mean 3 hourly hydrographs of the study catchments for the reference and future periods

Figure 4: Flow duration curves (FDCs) of the 3-hourly flow for the six study catchments both for the reference and future periods using bias corrected NorESM1-M (r1i1p1) global climate model, WRF regional climate model and RCP 8.5.

Figure 5. Distributions of the annual and seasonal maximum flow values of the 30 years period

Figures

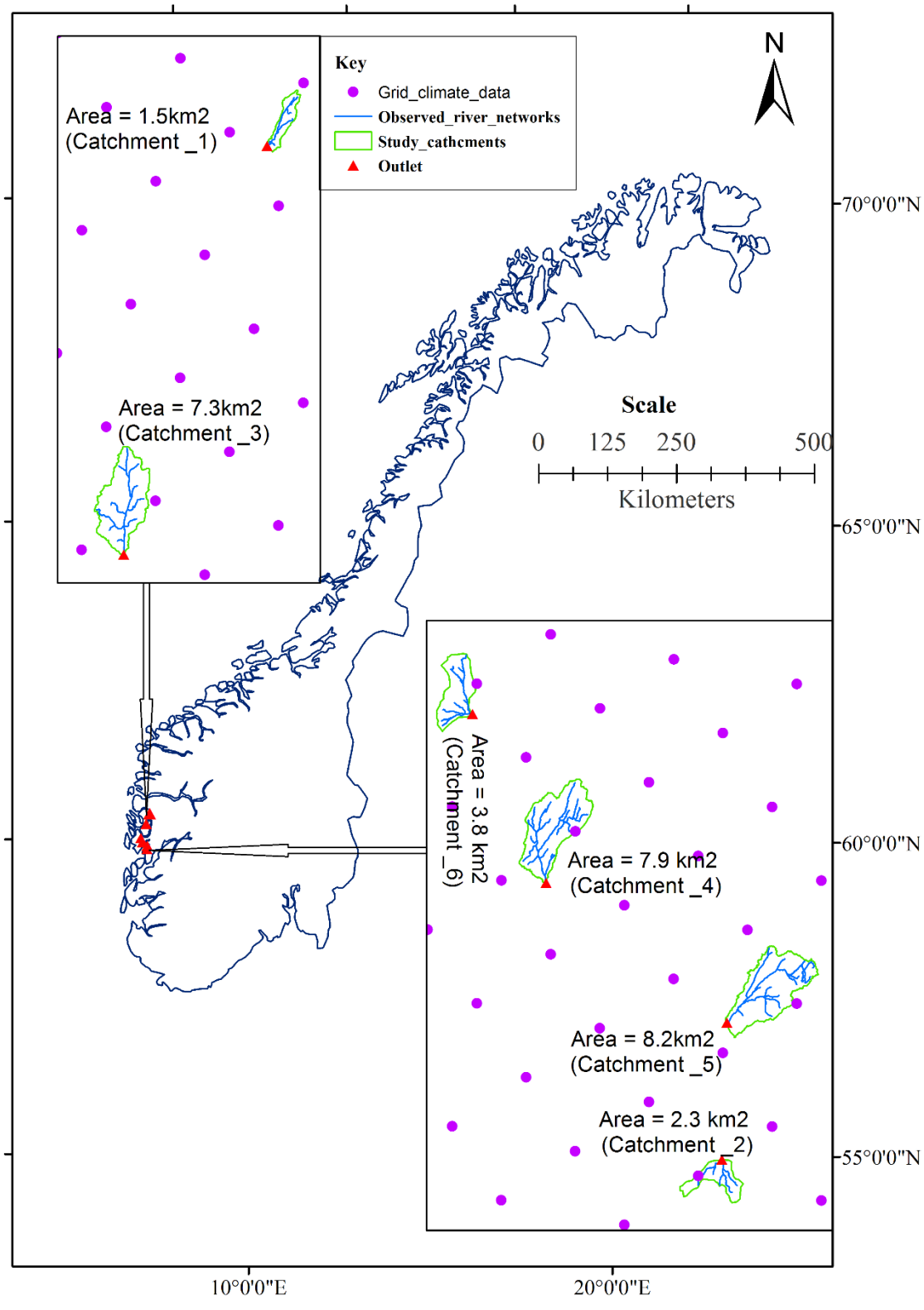

Figure 1. Locations of study catchments in Norway.

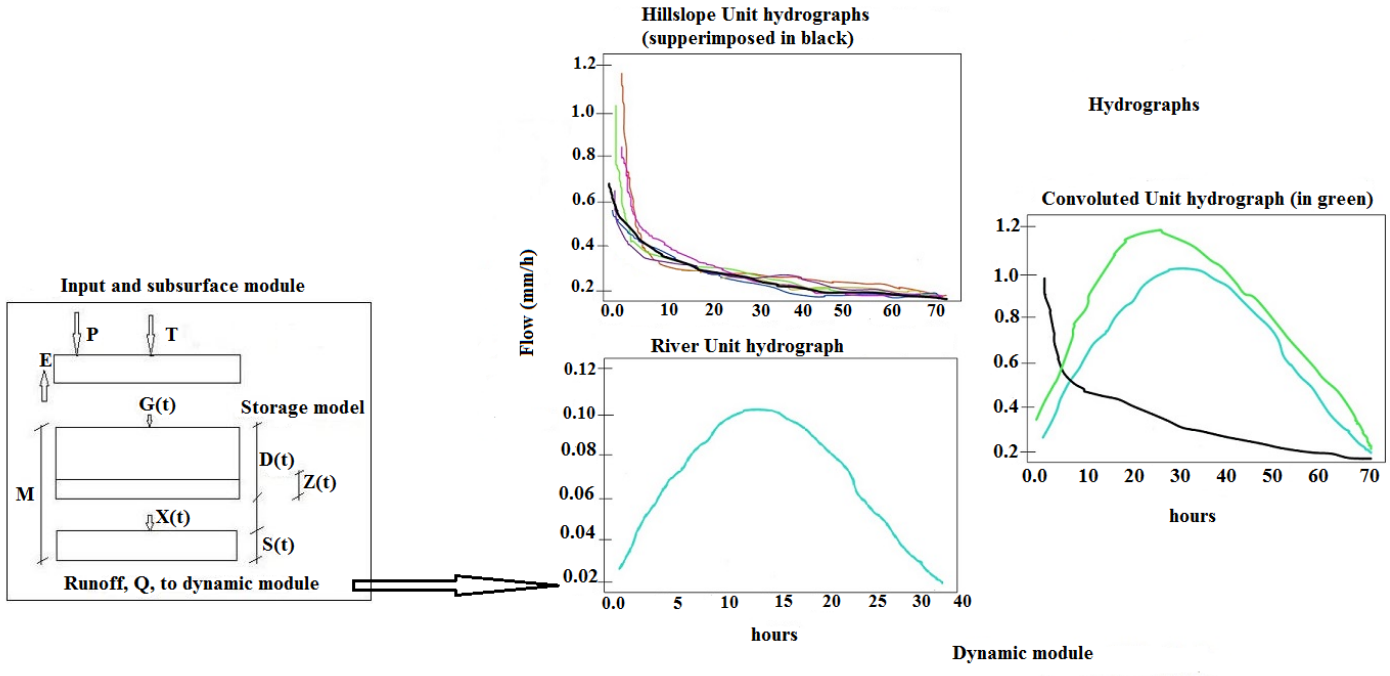

Figure 2. Structure of the Distance Distributions Dynamics model adapted from Skaugen and Onof (2014). Left panel: the storage model and right panel: hydrographs of hillslope and river. P is precipitation, T is temperature, E is actual evapotranspiration, G(t) is input from snowmelt and rain, Z(t) is soil moisture in unsaturated zone, X(t) is excess water, M is total volume of subsurface water reservoir, S(t) a saturated zone volume and D (t) is unsaturated zone volume.

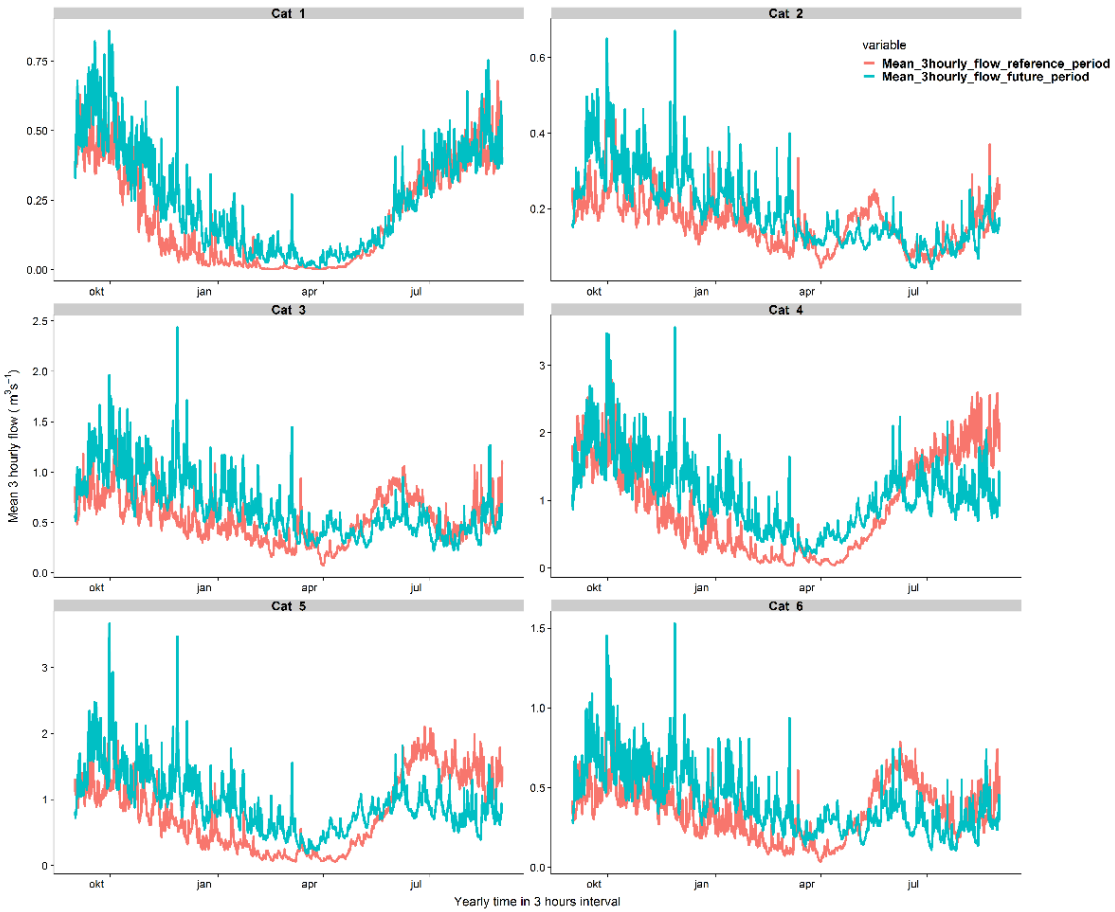

Figure 3. Yearly mean 3 hourly hydrographs of the study catchments for the reference and future period.

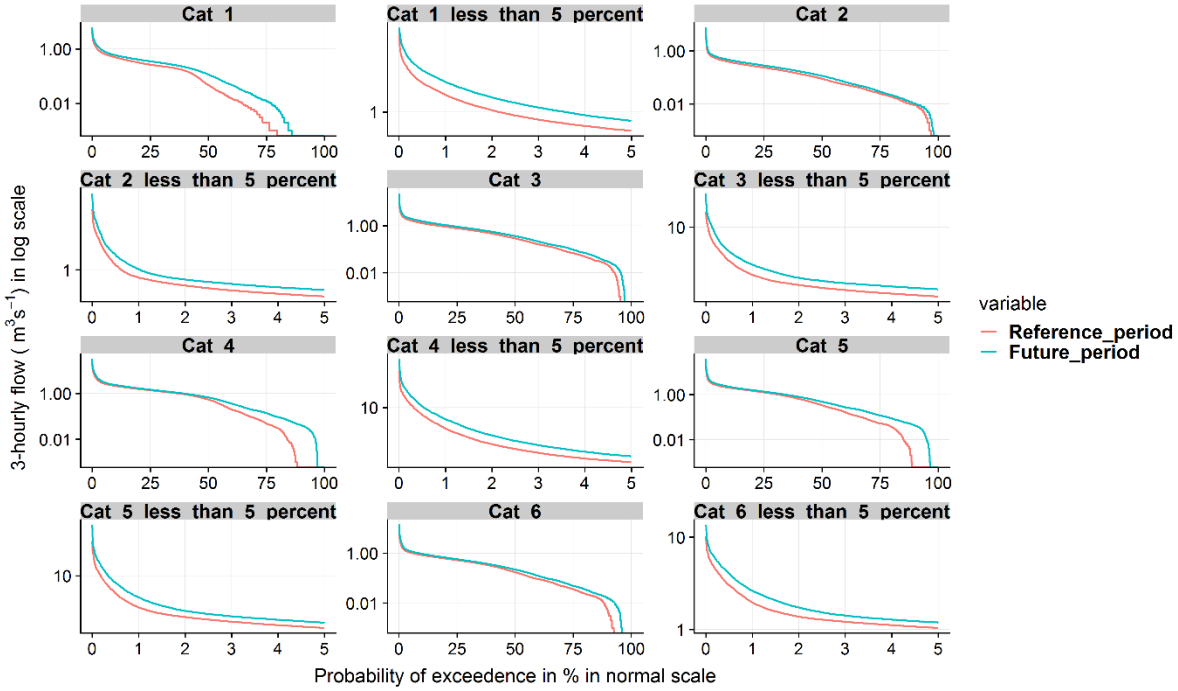

Figure 4: Flow duration curves (FDCs) of the 3-hourly flow for the six study catchments both for the reference and future period.

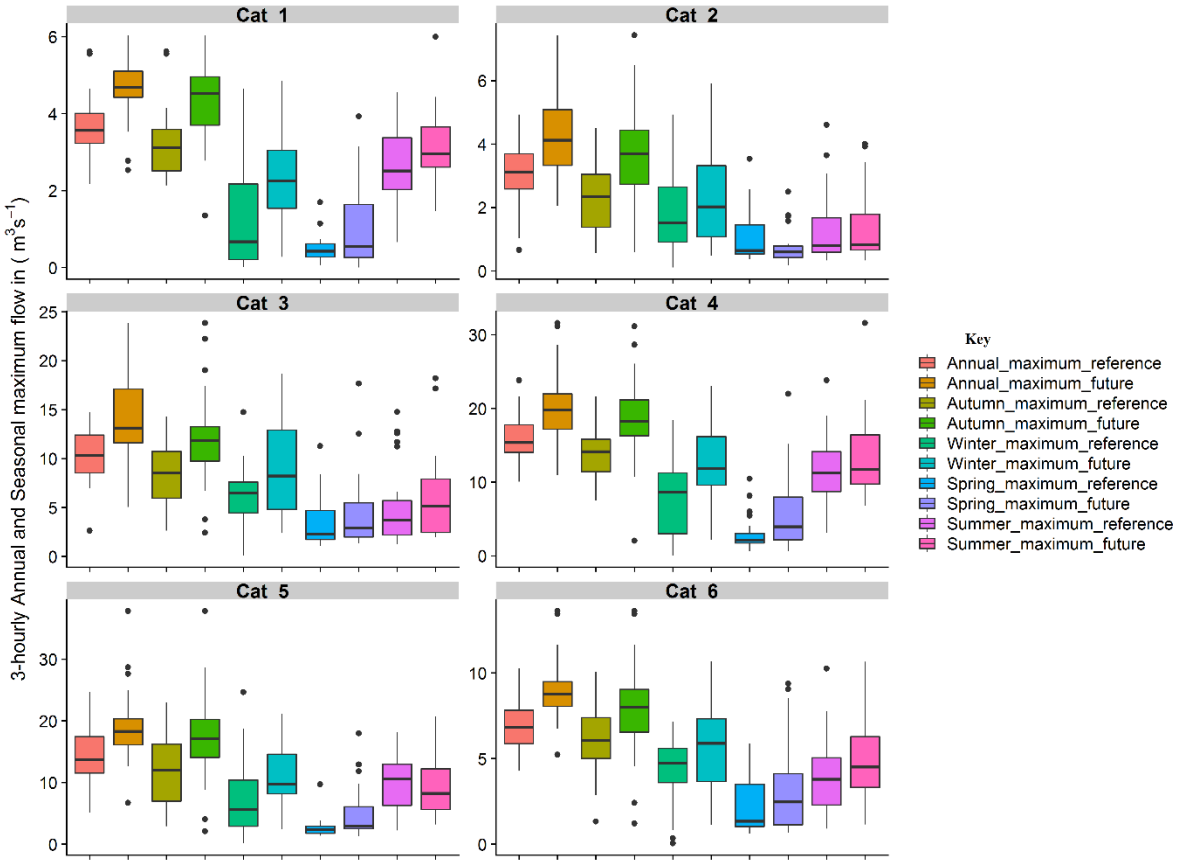

Figure 5. Distributions of the annual and seasonal maximum flow values of the 30 years period.

Tables

Table 1: Catchment descriptors of the study catchments

Catchments Descriptors	Unit	Symbol	Catchments					
			Cat_1	Cat_2	Cat_3	Cat_4	Cat_5	Cat_6
Mean of distance distributions of soils in the catchment to the nearest river reach	m	D_m	103.0	169.1	204.3	137.0	174.9	171.7
Mean of distance distributions of marsh land in the catchment to the nearest river reach	m	D_{mr}	0.0	261.0	220.7	109.9	107.2	154.3
Mean of distance distribution of points in the river to the outlet	m	D_r	1513.2	960.5	2671.2	3061.1	3402.8	1733.3
Catchment area	km^2	A	1.5	2.3	7.3	7.9	8.2	3.8
Effective lake	%	L_e	0.2	0.0	0.0	0.7	0.0	0.0
Forest	%	F	18.5	65.3	75.8	22.5	69.7	25.4
Bare mountain	%	B	79.6	27.6	14.8	66.0	18.9	65.3
Urban	%	U	0.0	0.1	0.0	0.0	0.0	0.0
Mean elevation	m	M_e	684.6	322.1	314.7	461.5	402.1	466.7
Mean anual precipitation	mm	M_p	3268.0	2243.0	2500.0	2781.0	2543.0	2644.0
Speciifc discharge	$l\ s^{-1}km^{-2}$	S_q	141.0	115.7	91.8	125.6	134.2	110.7
Mean river slope	$m\ km^{-1}$	R_s	162.6	266.2	88.4	106.4	118.6	154.9
Outlet location								
ETRS_1989_UTM_Zone_33N coordinate system (m)	Longtiude		-9376.0	-14513.6	-15886.7	-22440.2	-14280.8	-25871.8
	Latitude		6777231.6	6712810.0	6758694.5	6725236.5	6719015.4	6732970.8

Table 2: Coefficients of the power relation between D_m and A_c and the coefficients of determination (R-squared).

Catchment_ID	a	b	R-squared
Cat_1	1.42	0.41	0.97
Cat_2	0.87	0.45	0.99
Cat_3	0.87	0.46	1
Cat_4	1.2	0.44	0.99
Cat_5	0.99	0.45	1
Cat_6	0.87	0.46	1

Table 3: DDD model parameters of the study catchments estimated from regionalization

Model parameters needing regionalization	Catchments					
	Cat_1	Cat_2	Cat_3	cat_4	Cat_5	cat_6
Gshape	2.317	1.827	1.977	2.087	1.961	2.032
Gscale	0.041	0.036	0.034	0.033	0.038	0.037
GshInt	4.085	3.083	3.39	3.615	3.356	3.502
GscInt	0.018	0.016	0.015	0.015	0.017	0.017
fc	49.3	122.1	140.00	68.30	134.2	69.00
Pro	0.1	0.087	0.082	0.100	0.095	0.096
Cx	0.155	0.129	0.108	0.137	0.159	0.147
CFR	0.004	0.006	0.007	0.004	0.003	0.004
Cea	0.033	0.025	0.016	0.032	0.028	0.031
rv	1.22	1.240	1.17	1.200	1.260	1.190

Table 4: Changes of mean annual temperature and precipitation, mean annual maximum snow water equivalent (SWE) and mean annual evapotranspiration for all the study catchments using bias corrected NorESM1-M (r1i1p1) global climate model, WRF regional climate model and RCP 8.5.

Hydro-meteorological indicator	Unit	Change in indicator
Cat_1		
Mean annual precipitation	mm	22 %
Mean annual temprature	^{o}C	3.3 ^{o}C
Mean annual maximum SWE	mm	-78 %
Mean annual evapotranspiration	mm	63 %
Cat_2		
Mean annual precipitation	mm	24 %
Mean annual temprature	^{o}C	3.1 ^{o}C
Mean annual maximum SWE	mm	-48 %
Mean annual evapotranspiration	mm	67 %
Cat_3		
Mean annual precipitation	mm	24 %
Mean annual temprature	^{o}C	3.2 ^{o}C
Mean annual maximum SWE	mm	-50 %
Mean annual evapotranspiration	mm	43 %
Cat_4		
Mean annual precipitation	mm	20%
Mean annual temprature	^{o}C	3.2 ^{o}C
Mean annual maximum SWE	mm	-56 %
Mean annual evapotranspiration	mm	132 %
Cat_5		
Mean annual precipitation	mm	22 %
Mean annual temprature	^{o}C	3.2 ^{o}C
Mean annual maximum SWE	mm	-49 %
Mean annual evapotranspiration	mm	81 %
Cat_6		
Mean annual precipitation	mm	20.0 %
Mean annual temprature	^{o}C	3.0 ^{o}C
Mean annual maximum SWE	mm	-63.0 %
Mean annual evapotranspiration	mm	92 %

Table 5: Changes in percentage of mean annual flow and seasonal flows of the study catchments. The unit of the flows is m^3/s.

Hydrologic indicator (flow)	Change in indicator (%)	Hydrologic indicator (flow)	Change in indicator (%)
Cat_1		***Cat_4***	
Mean annual flow	33	Mean annual flow	17
Mean winter flow	256	Mean winter flow	168
Mean spring flow	49	Mean spring flow	100
Mean summer flow	4	Mean summer flow	-33
Mean Autumn flow	44	Mean Autumn flow	21
Cat_2		***Cat_5***	
Mean annual flow	22	Mean annual flow	19
Mean winter flow	41	Mean winter flow	147
Mean spring flow	-1	Mean spring flow	76
Mean summer flow	-7	Mean summer flow	-41
Mean Autumn flow	38	Mean Autumn flow	43
Cat_3		***Cat_6***	
Mean annual flow	22	Mean annual flow	17
Mean winter flow	68	Mean winter flow	81
Mean spring flow	4	Mean spring flow	10
Mean summer flow	-21	Mean summer flow	-35
Mean Autumn flow	41	Mean Autumn flow	35

Table 6: Winter/spring and fall centre of volume (CV) dates for the six study attachments

Annual timing	CV date (reference)	CV date (future)	Is CV date early or late?
Cat_1			
Winter/Spring	13 May	5 March	early
Fall	21 October	31 October	late
Cat_2			
Winter/Spring	18 March	2 March	early
Fall	11 November	12 November	late
Cat_3			
Winter/Spring	27 March	3 March	early
Fall	8 November	11 November	late
Cat_4			
Winter/Spring	24 April	10 march	early
Fall	29 October	8 November	late
Cat_5			
Winter/Spring	26 April	13 March	early
Fall	3 November	19 November	late
Cat_6			
Winter/Spring	11 April	3 March	early
Fall	8 November	11 November	late

Table 7: Changes in percentage of the mean annual and seasonal maximum flows in the future period compared to the reference period.

Annual and Seasonal maximum flows	Change in indicator (%)	Annual and Seasonal maximum flows	Change in indicator (%)
Cat_1		***Cat_4***	
Mean autumn maximum flow	38	Mean autumn maximum flow	33
Mean winter maximum flow	82	Mean winter maximum flow	60
Mean spring maximum flow	118	Mean spring maximum flow	106
Mean summer maximum flow	17	Mean summer maximum flow	18
Mean annual maximum flow	28	Mean annual maximum flow	29
Cat_2		***Cat_5***	
Mean autumn maximum flow	60	Mean autumn maximum flow	48
Mean winter maximum flow	32	Mean winter maximum flow	49
Mean spring maximum flow	-29	Mean spring maximum flow	86
Mean summer maximum flow	7	Mean summer maximum flow	1
Mean annual maximum flow	38	Mean annual maximum flow	31
Cat_3		***Cat_6***	
Mean autumn maximum flow	43	Mean autumn maximum flow	28
Mean winter maximum flow	46	Mean winter maximum flow	29
Mean spring maximum flow	25	Mean spring maximum flow	41
Mean summer maximum flow	21	Mean summer maximum flow	27
Mean annual maximum flow	37	Mean annual maximum flow	29

Table 8: Changes in the number of 3-hour floods which are greater than the minimum annual maximum flood in the reference period for all the study catchments.

Catchment ID	Mean annual number of 3-hours floods greater than the minimum annual maximum flood in the reference period		Changes in number (%)
	Reference period (1981-2011)	Future period (2070-2100)	
Cat_1	9.1	21.2	133.0
Cat_2	58	99.3	71.2
Cat_3	38	64.4	69.5
Cat_4	9	15.4	71.1
Cat_5	22.2	35.9	61.7
Cat_6	7	13.3	90

Table 9: Changes of flood frequencies with return periods of 2, 5, 10, 20, 25, 50, 100 and 200 years between the future and reference periods using Gumbel's Extreme Value Distribution for all study catchments.

T(years)	Change (%)					
	Cat_1	**Cat_2**	**Cat_3**	**Cat_4**	**Cat_5**	**Cat_6**
2	29	37	36	28	31	30
5	24	36	38	33	31	27
10	22	36	39	36	31	26
20	20	35	40	38	31	25
25	20	35	40	39	31	25
50	18	35	41	40	31	24
100	17	35	41	42	31	23
200	16	35	41	43	31	23